Journal of King Saud University – Engineering Sciences (2013) xxx, xxx–xxx

King Saud University

Journal of King Saud University – Engineering Sciences

www.ksu.edu.sa
www.sciencedirect.com

ORIGINAL ARTICLE

Natural fiber composite design and characterization for limit stress prediction in multiaxial stress state

Christopher C. Ihueze [a], Christian E. Okafor [a,*], Chris I. Okoye [b]

[a] Department of Industrial and Production Engineering, Nnamdi Azikiwe University, Awka, Nigeria
[b] Department of Mechanical Engineering, Nnamdi Azikiwe University, Awka, Nigeria

Received 21 January 2013; accepted 21 August 2013

KEYWORDS

Multiaxial stresses;
Composites;
Natural fibers;
Yield stress;
Plantain fibers

Abstract This paper focuses on the design of natural fiber composites and analysis of multiaxial stresses in relation to yield limit stresses of composites loaded off the fibers axis. ASTM D638-10 standard for tensile test was used to design and compose composites of plantain fiber reinforced polyester (PFRP). While the rule of mixtures was used in the evaluation of properties of composites in the fiber direction the evaluation of properties perpendicular or transverse to the fiber direction was done based on the value of the orthogonal stresses evaluated using ANSYS finite element software, the application of the Brintrup equation and Halpin–Tai equation. The yield strength for the plantain empty fruit bunch fiber reinforced polyester resin (PEFBFRP) was estimated as 33.69 MPa while the yield strength of plantain pseudo stem fiber reinforced polyester resin (PPSFRP) was estimated as 29.24 MPa. Above all, the PEFBFRP with average light absorbance peak of 45.47 was found to have better mechanical properties than the PPSFRP with average light absorbance peak of 45.77.

1. Introduction

Natural fibers are found within the lignocelluloses and are made up of cellulose, hemicelluloses, pectin, lignin, and water mainly (Rowell et al., 1998; Westman et al., 2010). The application of natural fibers to component design through polymers is limited by hydrophilic nature of the cellulose.

Though disadvantages exist for property enhancement through polymer matrix reinforcement, natural fiber composites have comparable specific properties with glass fiber components and even better specific weight than glass fiber components (Westman et al., 2010). The major setbacks for natural fiber composites are high water absorption of the fibers and poor wettability of the inorganic fiber with the organic matrix. However, classical reports on modification of natural fibers to improve on the wettability and hydrophilicity of natural fibers exist (Ghali et al., 2011).

A designer is always interested in the estimation of failure stresses of the material he wants to employ in his design and the most important characteristics requiring consideration

* Corresponding author. Tel.: +234 8033622498.
E-mail addresses: cc.ihueze@unizik.edu.ng (C.C. Ihueze), cacochris33@yahoo.com, chrisok222@gmail.com (C.E. Okafor).

Peer review under responsibility of King Saud University.

ELSEVIER Production and hosting by Elsevier

1018-3639 © 2013 Production and hosting by Elsevier B.V. on behalf of King Saud University.
http://dx.doi.org/10.1016/j.jksues.2013.08.002

for most engineering components include, mechanical properties (strength, stiffness, specific strength and stiffness, fatigue and toughness, and the influence of high or low temperatures on these properties), corrosion susceptibility and degradation, wear resistance and frictional properties, special properties (for example, thermal, electrical, optical and magnetic properties, damping capacity, etc.), molding and/or other methods of fabrication and the total costs attributable to the selected material and manufacturing route.

High cost of synthetic fibers and health hazards of asbestos fibers have really necessitated the exploration of natural fibers (Agbo et al., 2009; Brahmakumar et al., 2005). Consequently, natural fibers have always formed wide applications from the time they gained commercial recognition (Samuel et al., 2012). Stamboulis and Baley, 2001 reported that this excellent price-performance ratio at low weight in combination with the environmentally friendly character is very important for the acceptance of natural fibers in large volume engineering markets, such as the automotive and construction industries. Oladele et al. (2010) reported that the fiber/matrix has an important role in the micromechanical behavior of composite.

Plantain production in Africa is estimated at more than 50% of worldwide production (Food and Organization, 1990). Nigeria is one of the largest plantain producing countries in the world (Food and Organization, 2006). It is estimated that over 15.07 million tons of plantain is produced every year in Nigeria (Ahmed, 2004). Furthermore, plantain grows to its mature size in only 10 months, whereas wood takes a minimum of 10 years (Xiaoya et al., 1998).

The fiber from the plantain empty fruit bunch and pseudo stem that are nowadays disposed as an unwanted waste, might be seen as a recyclable potential alternative to be used in polymeric matrix composite material (Satynarayana et al., 1987; Venkataswamy et al., 1987; Calado et al., 2000). The plantain plant (Musa Spp Acuminata) is a multivalent fiber producer, its fibers can be extracted from any part of the plant including the long leaf sheet and the pseudo-stem (Venkataswamy et al., 1987).

Hinton et al., 2004 reported the need for reliable multiaxial or even biaxial experimental data to validate failure theories. ''Multiaxial'' and biaxial testing of composites was studied in Chen and Matthews (1993), but a careful examination of (Olsson, 2011) submissions clarifies that ''multiaxial'' solely refers to various combinations of in-plane loads. Crawford, 1998 reported the rule of mixture equation, the Halpin–Tsai equation and the Brintrup equation for the estimation of composite modulus. Found in almost all the strength of materials and mechanical design tests are relevant equations for the prediction of failure of engineering materials.

Many factors must be considered when designing fiber reinforced composite (Hall, 1981). These factors include volume fraction of fibers, aspect ratio of fiber and fiber orientation in matrix etc. A multiaxial stress state can be a biaxial or triaxial stress state. In practice it is difficult to devise experiments to cover every possible combination of critical stresses because each test is expensive and a large number is required. Therefore a theory is needed that compares the normal and shear stresses σ_x, σ_y, σ_z, τ_{xy}, τ_{yz} and τ_{xz} with the uniaxial stress for which experimental data are relatively easy to obtain (Hamrock et al., 1999).

Experimental results from the World Wide Failure Exercise (WWFE) Hinton and Soden, 2002; Soden et al., 2002 indicate that the (admittedly scarce) data on fiber tensile failure under bi-or multi-axial stress states do not seem to invalidate the maximum stress criterion. Kaleemulla and Siddeswarappa (Hinton et al., 2004) investigated the influence of fiber orientation and fiber content of epoxy resin components on mechanical prosperities. Chimekwene et al., 2012 conducted studies on plantain empty fruit bunch fiber reinforced epoxy composite laminates. Okafor et al., 2013 conducted many designed experiments on the measurement of the mechanical properties such as tensile strength, flexural strength, hardness strength and impact strength of plantain fiber reinforced polyester resin.

Haj-Ali and Kilic, 2002; Kilic and Haj-Ali, 2003 investigated the nonlinear behavior of thick-section and multi-layered FRP composites and proposed non-linear macro- and micro-mechanical models. Their models were able to reasonably capture the multiaxial response. El-Hajjar and Haj-Ali, 2004 proposed a testing method to measure the in-plane shear response of FRP composites under multi-axial deformation using a modified Arcan test fixture. Mittal, 2000; Haj-Ali and Muliana, 2003; Haj-Ali and Muliana, 2004 have proposed constitutive models to generate the nonlinear mechanical and time-dependent behavior of the FRP composite. This study tends to focus on relevant laminate theory in the design and analysis of composite stresses, it offers an integrated micromechanical approach and relevant ASTM standard in composite design. Detailed visualization of material responses to real-world forces is carried out using the Finite Element Analysis (FEA) model.

Nowadays, the application of polymer composites as engineering materials is fast becoming state of the art, it follows that the ability of the engineer to design for the characteristics of polymer composites is an important advantage. The problem of this study therefore is to develop a new class of composite material and establish a design criterion (multi axial stress predictive models), which can generate the yield stresses of plantain fiber reinforced composite for the determination of occurrence of yielding; the failure prediction of this study is based on the experimental results of Okafor et al., 2013 and the application of classical equations on the prediction of failure of material as well as the application of finite element analysis software to estimate the orthogonal stresses that are used in the evaluation of the principal stresses.

2. Theoretical formulations and composite design

2.1. Composite volume and moduli

The volume of composites and moduli are evaluated following the rule of mixtures and classical empirical relations. By writing volume fraction of fibers as

$$V_{\mathrm{fr}} = \frac{V_f}{V_c} = \frac{V_f}{V_f + V_R} \tag{1}$$

$$V_R = \left(\frac{1 - V_{fr}}{V_{fr}}\right) V_f \tag{2}$$

Also by involving density ratios

$$\frac{M_{f2}}{V_{f2}} = \frac{M_f}{V_f} \tag{3}$$

where

V_{fr} = volume fraction of fibers, V_f = actual volume of fibers related to composition and volume fraction, V_c = volume of composite related to molding and approximately equal to volume of mold for specific test, V_{f2} = volume of fibers of a measurable mass determined through application of Archimedes principle, V_R = volume of resin or matrix material, M_{f2} = mass of fibers determined through application of Archimedes principle.

From Eq. (1)

$$V_f = V_{fr} V_c \tag{4}$$

and from Eq. (3)

$$M_f = \frac{M_{f2}}{V_{f2}} V_f = \frac{M_{f2}}{V_{f2}} (V_{fr} V_c) \tag{5}$$

Next is to determine the mass of resin for specific composition of a certain volume fraction by the expression,

$$M_c = M_f + M_R \tag{6}$$

By knowing the density of resin as ρ_R, the mass of resin for making a composite of a particular volume fraction can be expressed as

$$\rho_R = \frac{M_R}{V_R}, M_R = V_R \rho_R \tag{7}$$

V_c is determined with the expected number of replicate samples and the depth of the mold as specified by ASTM standard in mind. Remember also that for a particular volume fraction computations of V_f, M_f and M_R are made.

Composites are usually weaker in direction transverse to the fiber direction. Generally the fibers are dispersed at random on any cross section of the composite and so the applied force will be shared by the fibers and matrix but not necessarily equally as assumed in the rule of mixtures. Eq. (8) is derived for composite modulus in the transverse direction following the rule of mixture assumption.

$$\frac{1}{E_2} = \frac{V_{fr}}{E_f} + \frac{V_{mr}}{E_m} \tag{8}$$

$$E_2 = \frac{E_f E_m}{V_{fr} E_m + V_{mr} E_f} \tag{9}$$

Other inaccuracies also arise due to mis-match of Poisson's ratios for the fibers and matrix. These issues led to some other empirical equations to estimate composite modulus. One of these is the Halphin–Tsai equation which is expressed as

$$E_2 = E_m \left(\frac{1 + 2\beta V_{fr}}{1 - \beta V_{fr}} \right) \tag{10}$$

where

$$\beta = \frac{(E_f/E_m) - 1}{(E_f/E_m) + 2} \tag{11}$$

An alternative equation for the modulus of composite is the Brintrup equation which is expressed as

$$E_2 = \frac{E'_m E_f}{E_f(1 - V_{fr}) + V_{fr} E'_m} \tag{12}$$

where

$E'_m = E_m/(1 - v_m^2)$ and v_m is Poisson's ratio of matrix material.

2.2. Fiber orientation and fiber stress distribution in loading off the fiber axis

This is for the analysis of composites with fibers inclined or oriented with respect to the axial or longitudinal direction of the composite. It applies to situation where the applied loading axis does not coincide with the fiber axis. The first step in the analysis of this situation is the transformation of the applied stresses on the fiber axis. By referring to Fig. 1, it may be seen that σ_x and σ_y may be resolved into x, y axes as follows:

$$\sigma_1 = \sigma_x \cos^2\theta + \sigma_y \sin^2\theta + 2\tau_{xy} \sin\theta \cos\theta \tag{13}$$

$$\sigma_2 = \sigma_x \sin^2\theta + \sigma_y \cos^2\theta - 2\tau_{xy} \sin\theta \cos\theta \tag{14}$$

$$\tau_{12} = -\sigma_x \sin\theta \cos\theta + \sigma_y sin\theta \cos\theta + \tau_{xy}(\cos^2\theta - \sin^2\theta) \tag{15}$$

where

σ_1 = stress parallel to the fiber axis or longitudinal stress, σ_2 = stress perpendicular or transverse to the fiber axis or the transverse stress.

By putting Eqs. (13)–(15) in matrix form,

$$\begin{Bmatrix} \sigma_1 \\ \sigma_2 \\ \tau_{12} \end{Bmatrix} = \begin{bmatrix} c^2 & s^2 & 2sc \\ s^2 & c^2 & -2sc \\ -sc & sc & (c^2 - s^2) \end{bmatrix} \begin{Bmatrix} \sigma_x \\ \sigma_y \\ \tau_{xy} \end{Bmatrix} \tag{16}$$

where $c = cos\theta$ and $s = sin\theta$

Eq. (16) can also be expressed as

$$\{\sigma\}_{12} = [T_\sigma]\{\sigma\}_{xy} \tag{17}$$

where $[T_\sigma]$ is called the stress transformation matrix. Similar transformations may be made for the strains so that

$$\begin{Bmatrix} \varepsilon_1 \\ \varepsilon_2 \\ \frac{1}{2}\gamma_{12} \end{Bmatrix} = [T_\sigma] \begin{Bmatrix} \varepsilon_x \\ \varepsilon_y \\ \frac{1}{2}\gamma_{xy} \end{Bmatrix} \tag{18}$$

Finite element analysis is very useful in the computation of the stresses' distribution within the global axes. It is only when these stresses σ_x and σ_y and τ_{xy} are known that computation of the transverse and directional properties such as σ_1, σ_2 and τ_{12} can be evaluated.

The shear modulus, elastic modulus and Poisson's ratio are related as

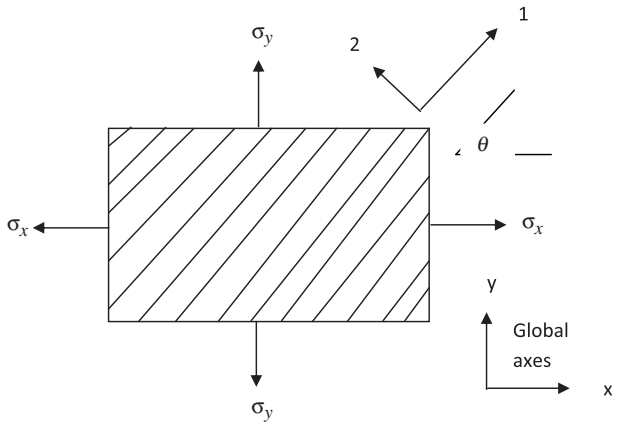

Figure 1 Single thin composite lamina under plane stress.

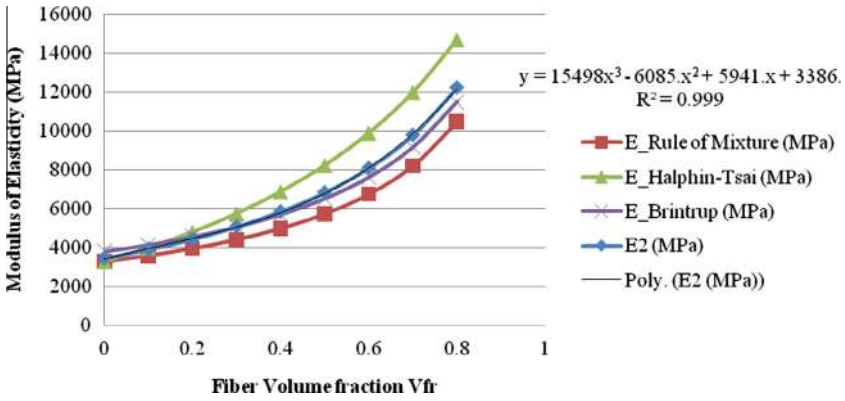

Figure 2 Depiction of PPSFRP transverse modulus computed with classical equations.

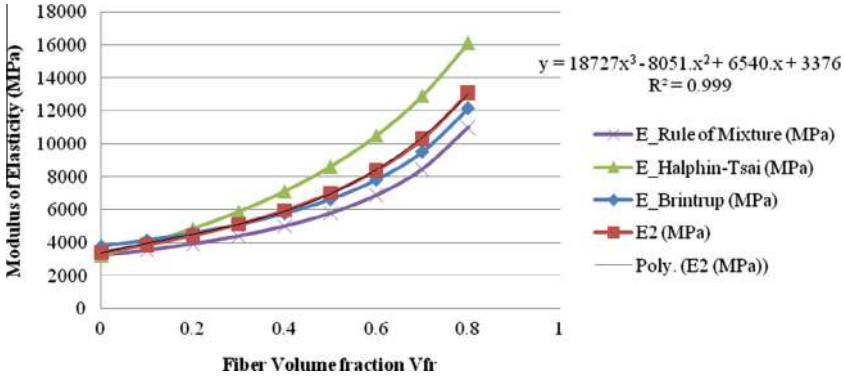

Figure 3 Depiction of PEFBFRP transverse modulus computed with classical equations.

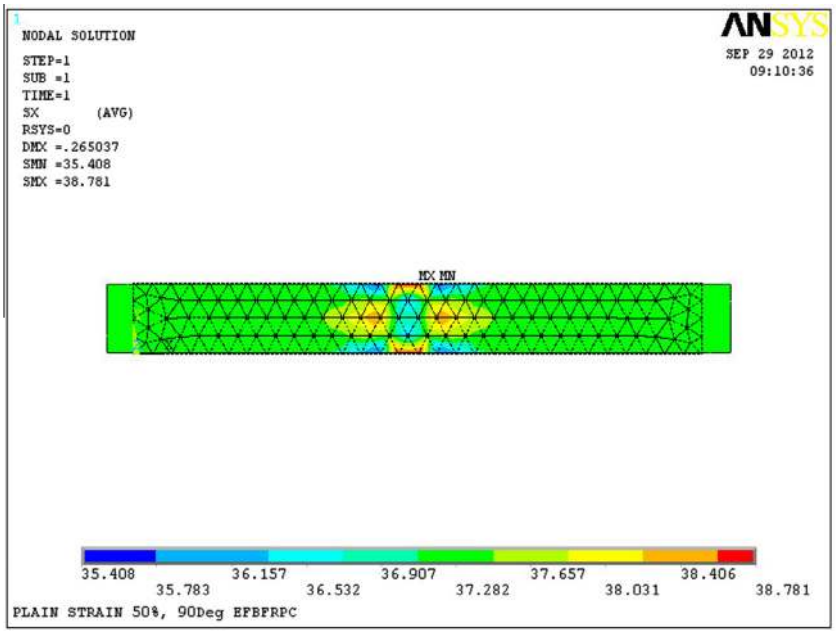

Figure 4 Plane strain analysis for PEFBFRP showing distribution of applied stress in *x*-direction with a maximum stress of 38.772 MPa.

Please cite this article in press as: Ihueze, C.C. et al., Natural fiber composite design and characterization for limit stress prediction in multiaxial stress state. Journal of King Saud University – Engineering Sciences (2013), http://dx.doi.org/10.1016/j.jksues.2013.08.002

$$G = \frac{E}{2(1+\nu)} \tag{19}$$

While the shear stress and shear modulus are related as

$$\tau = \frac{G}{2\pi} \tag{20}$$

2.3. Yielding of composite materials

A designer is always conscious of the failure of material of construction that he specifies limit stresses to be applied to field materials. The stresses applied to the material in service are not expected to exceed the ultimate strength of the material usually provided in a material data sheet.

If an isotropic material is subjected to multi-axial stresses such as σ_x, σ_y and σ_z then the situation is slightly more complex but there are well established procedures for predicting failure. If σ_x, σ_y and σ_z are applied, it is not only a question of ensuring that neither of these exceeds $\hat{\sigma}_T$; at values of σ_x, σ_y and σ_z below $\hat{\sigma}_T$ there can be a plane within the material where the stress reaches $\hat{\sigma}_T$ and this will initiate failure.

The stresses acting on the three principal planes of a stressed material element need to be known before yielding can be predicted for a general case of engineering material.

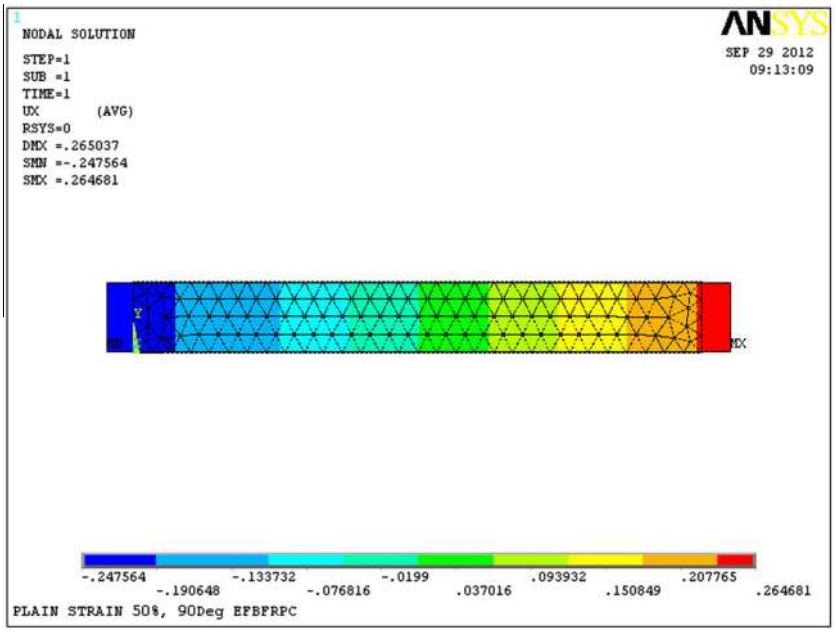

Figure 5 Plane strain analysis for PEFBFRP resulting to a displacement of 0.264681 mm.

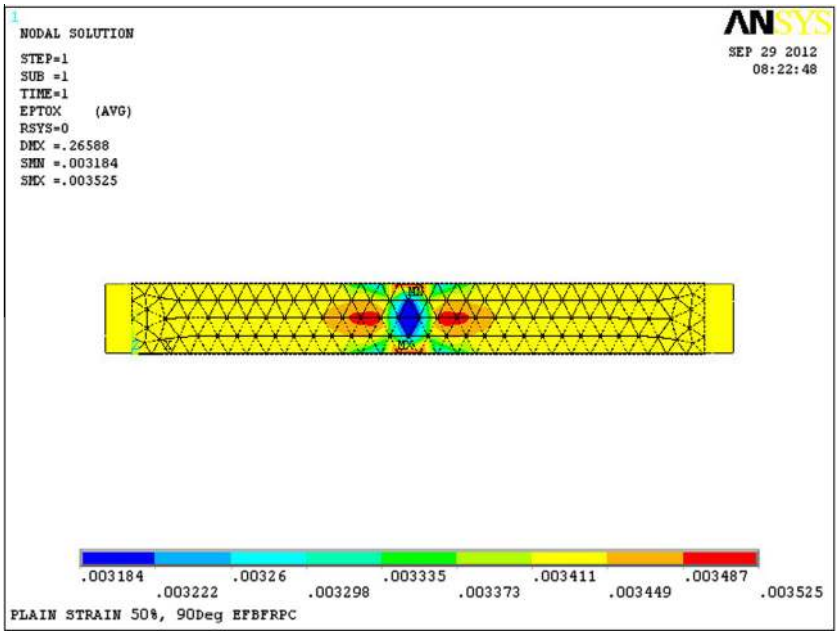

Figure 6 Plane strain analysis for PEFBFRP resulting to strain of 0.003525.

The classical relation for predicting the three principal stresses in a triaxially stressed state is expressed in Hamrock et al. (1999) and Shigley and Mischke (1989) as

$$\sigma^3 - (\sigma_x + \sigma_y + \sigma_z)\sigma^2 + (\sigma_x\sigma_y + \sigma_x\sigma_z + \sigma_y\sigma_z - \tau_{xy}^2 - \tau_{yz}^2 - \tau_{zx}^2)\sigma - (\sigma_x\sigma_y\sigma_z + 2\tau_{yz}\tau_{zx} - \sigma_x\tau_{yz}^2 - \sigma_y\tau_{zx}^2 - \sigma_z\tau_{xy}^2) = 0 \quad (21)$$

Solving the three roots of this equation gives the value of the three principal stresses as σ_1, σ_2, and σ_3 where $\sigma_1 \geqslant \sigma_2 \geqslant \sigma_3$.

The principal shear stresses are determined with the relations

$$\tau_{1/2} = \frac{\sigma_1 - \sigma_2}{2}, \tau_{2/3} = \frac{\sigma_2 - \sigma_3}{2}, \tau_{1/3} = \frac{\sigma_1 - \sigma_3}{2} \quad (22)$$

A good knowledge of the principal stresses on the element of material enables the designer to apply the appropriate theory of failure for the material of his design. Some of the failure theories are the maximum shear stress theory (MSST), the distortion energy theory (DET), and the maximum normal stress theory (MNST).

The maximum shear stress theory (MSST) also remembered as Tresca yield criterion is well suited in predicting failure of ductile materials. This Tresca yield criterion is expressed as

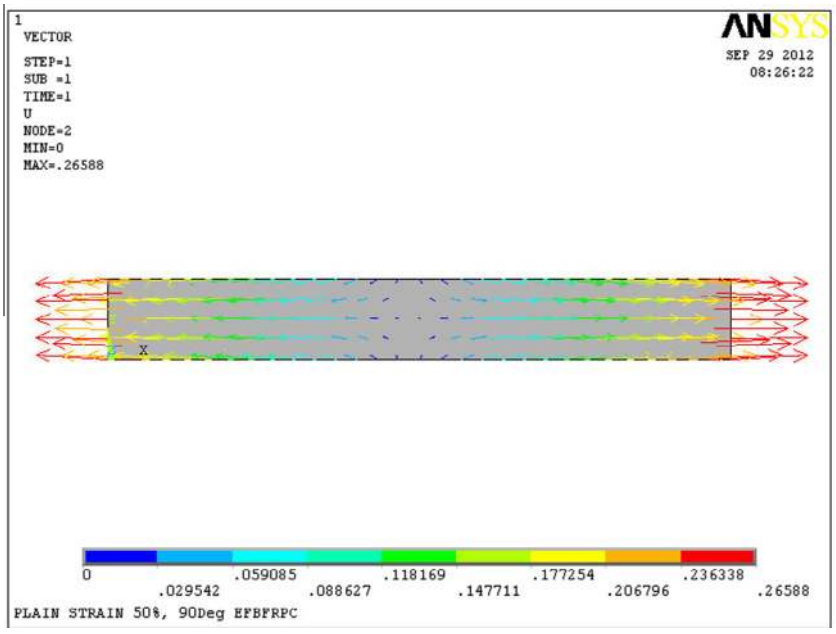

Figure 7 Vector plots depiction of degree of freedom for PEFBFRP.

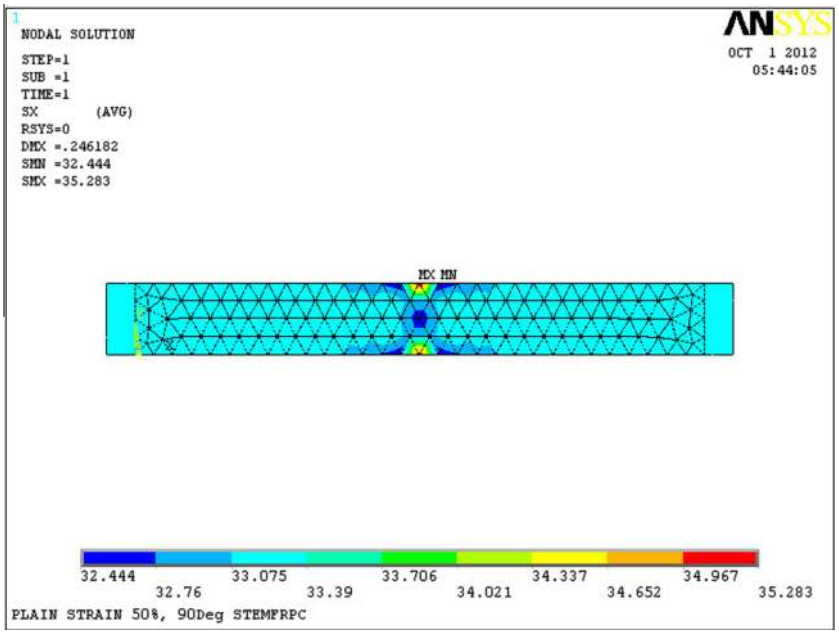

Figure 8 Plane strain analysis for PPSFRP showing distribution of applied stress in x-direction with a maximum stress of 35.283 MPa.

$$\sigma_1 - \sigma_3 = S_y or \tau_{max} \geq \frac{S_y}{2} \quad (23)$$

where S_y is the yield stress of the material.

The distortion energy theory (DET) also known as the von Mises criterion, postulates that failure is caused by the elastic energy associated with shear deformation. The von Mises stress is expressed as

$$\sigma_e = \frac{1}{\sqrt{2}}\sqrt{(\sigma_1 - \sigma_2)^2 + (\sigma_2 - \sigma_3)^2 + (\sigma_3 - \sigma_1)^2} \quad (24)$$

Thus DET predicts failure if

$$\sigma_e = S_y \quad (24b)$$

The maximum normal stress theory (MNST) states that failure occurs at the ultimate stress of the material. This can be expressed as

$$\sigma_1 \geq S_{ut}/n_s, \sigma_3 \geq S_{uc}/n_s \quad (25)$$

where

S_{ut} = uniaxial ultimate stress in tension, S_{uc} = uniaxial ultimate stress in compression, n_s = safety factor.

3. Methodology

This involves a presentation of the composite design process for fiber reinforced composites, the application of empirical relation in the determination of the directional moduli of

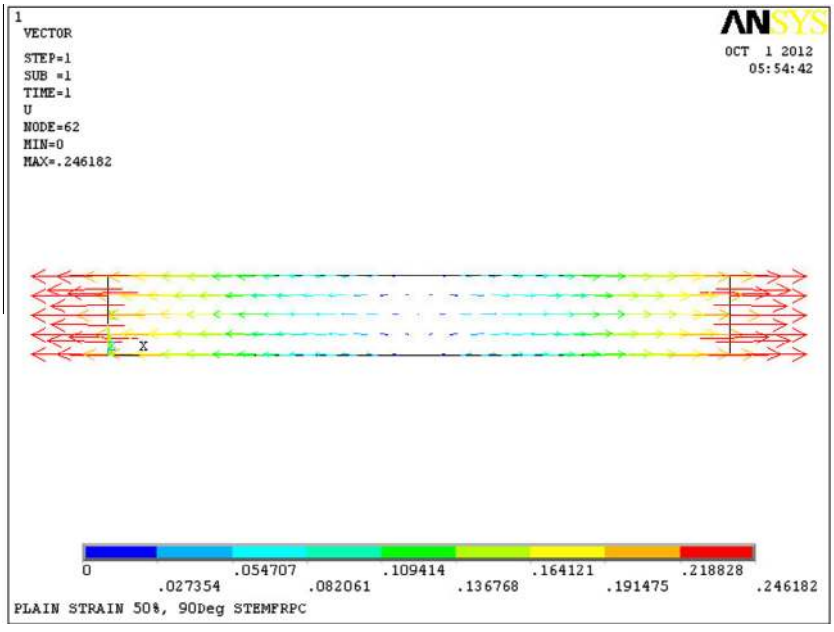

Figure 9 Vector plot depiction of degree of freedom for PPSFRP.

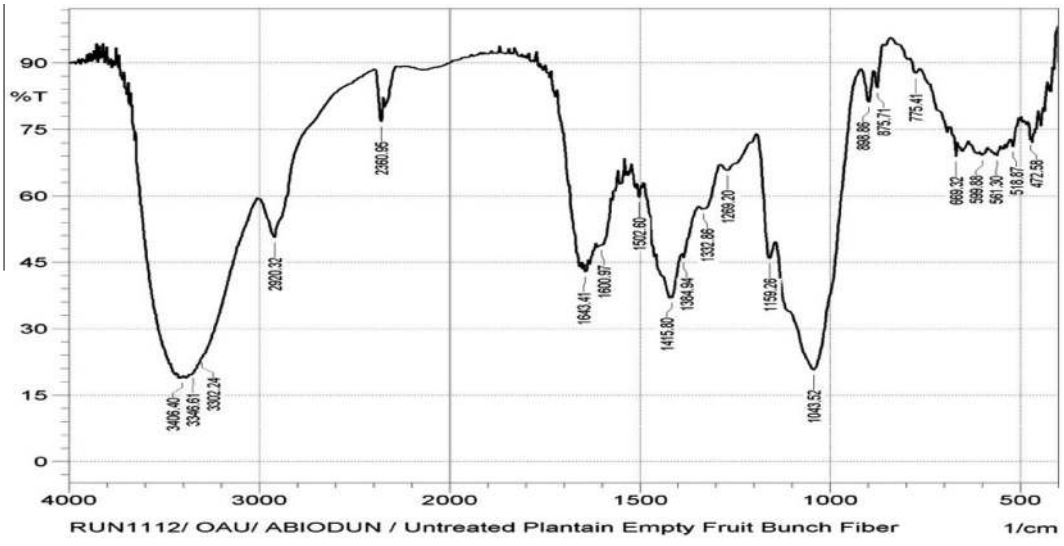

Figure 10 FTIR spectra of untreated plantain EFB fibers.

aligned fiber composites, the determination of principal stresses associated with three principal planes of a stressed composite element using the finite element ANSYS software in the estimation of applied orthogonal stresses, and the prediction of composite yield stress for composites of plantain fiber reinforced composites using experimental results of Okafor et al., 2013.

3.1. Design of composites for various mechanical tests

The ASTM standards for various mechanical tests of plastics are presented in Table 1.

The volume of composite is designed with specifications of Table 1. By considering a mold size of $300 \times 300 \times 12$ mm that is suitable for flexural, tensile, hardness and Charpy impact tests, the composite volume is designed with specifications of Table 1 for tensile testing.

The volume of fibers V_f is computed by Eq. (4) so that by considering volume fraction $V_{fr} = 0.10-0.80$, and tensile testing standard, the parameters needed for safe design and analysis of PFRP composites are evaluated with relevant equations already established in this study and presented in Tables 3 and 4.

3.2. Design for composite modulus

Composites are weaker in directions perpendicular to fiber direction (transverse direction) and stronger in directions

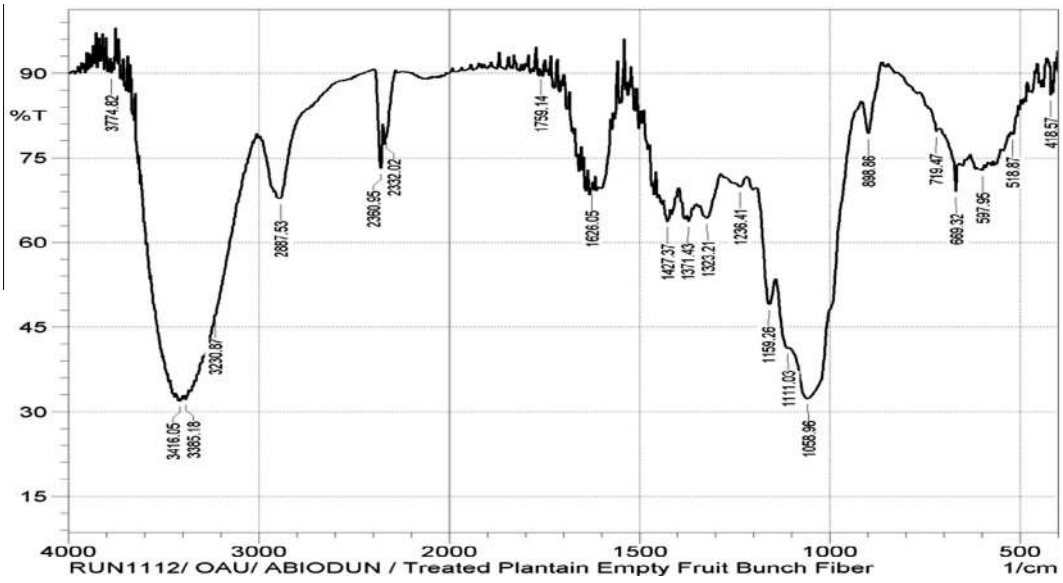

Figure 11 FTIR spectra of treated plantain empty fruit bunch fibers.

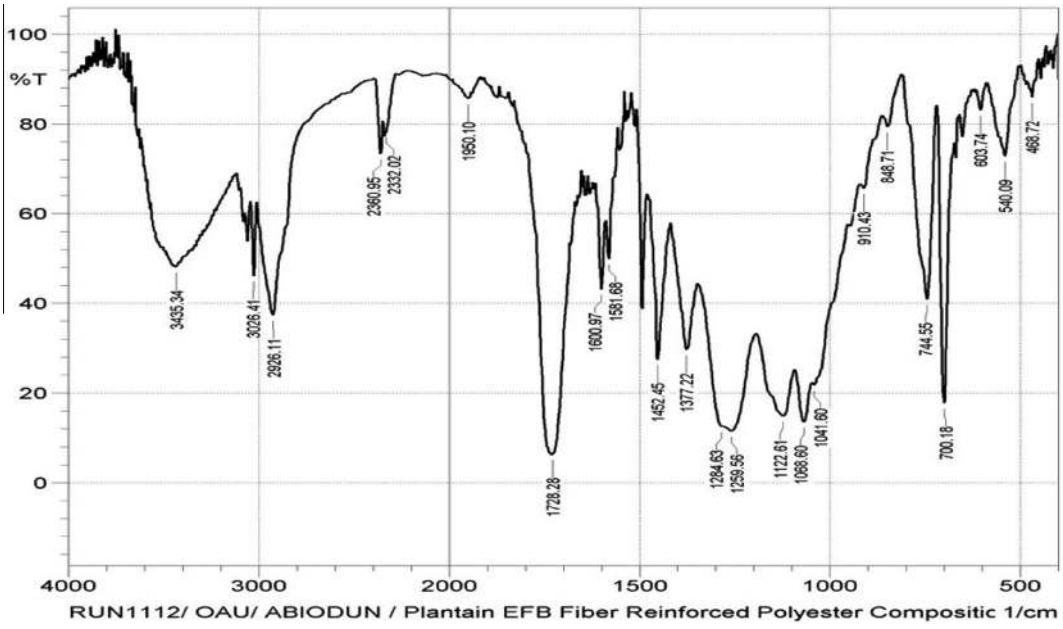

Figure 12 FTIR spectra of plantain EFB fiber reinforced composites.

Please cite this article in press as: Ihueze, C.C. et al., Natural fiber composite design and characterization for limit stress prediction in multiaxial stress state. Journal of King Saud University – Engineering Sciences (2013), http://dx.doi.org/10.1016/j.jksues.2013.08.002

parallel to the fiber axis. Most longitudinal properties of unidirectional fiber composites are evaluated by equation from rule of mixtures. Such properties include, the longitudinal modulus, tensile strength of composite, density of composite, Poisson's ratio of composite, shear modulus, thermal conductivity of composite etc. (Crawford, 1998). The mechanical properties of fibers and polyester resins of this study are presented in Tables 5 and 6.

The longitudinal modulus of unidirectional fiber composites can be estimated using the rule of mixture equation.

$$E_1 = E_f V_{fr} + E_{rm} V_{rm} \tag{26}$$

3.3. Estimation of transverse modulus of composite

The average value of modulus computations from Eqs. 9, 11, and 12 using data of Tables 5 is presented in Figs. 7 and 8, the average modulus E_2 estimated for PPSFRP and PEFBFRP composites at 50% volume fraction of fibers are 6817.586 and 7030.962 MPa, respectively.

Figs. 1 and 2 express the variation of transverse moduli of composites with volume fraction of fibers while giving the average values of transverse moduli at 50% volume fraction estimated with rule of mixtures, Brintrup and Halpin–Tai equations as 6818 and 7031 MPa, respectively for PPSFC and PEFBFRC.

Therefore a computational model for evaluating the elastic modulus of plantain pseudo stem fiber reinforced polyester matrix based material is expressed as

$$E_2 = 15498 V_{fr}^3 - 6085 V_{fr}^2 + 5941 V_{fr} + 3386$$

Through Fig. 2 a cubic polynomial equation relating elastic modulus and volume fraction was established in this study for plantain EFBFRC as

$$E_2 = 18727 V_{fr}^3 - 8051 V_{fr}^2 + 6540 V_{fr} + 3376$$

3.4. Estimation of random modulus of composite

This is based on the rule of mixture assumptions and Eq. (27). The rule of mixture states that the modulus of a unidirectional fiber composite is proportional to the volume fraction of the materials in the composite. The modulus of elasticity varies with direction because of inclination of the fibers such that the substantive modulus of elasticity is

$$E = E_r = E_1 + E_2 = E_{random} = 3E_1/8 + 5E_2/8 \tag{27}$$

From rule of mixtures,

$$E_1 = E_f \times V_{fr} + E_m \times V_{rm} \tag{28}$$

E_2 is regarded as the transverse modulus of the aligned fiber composite and is determined according to Eqs. (10)–(12).

The shear modulus of the composite is determined with

$$G_{random} = \frac{1}{8} E_1 + \frac{1}{4} E_2 \tag{29}$$

Poisson's ratio of aligned fiber composites is estimated with

$$v_{random} = \frac{E_r}{2G_r} - 1 \tag{30}$$

Since the dispersions of fibers in the cross section of unidirectional composites it at Radom (Crawford, 1998).

For plantain stem fiber reinforced composites, where E_f, V_{fr}, E_{rm}, V_{rm} = 23555 MPa, 0.5, 2500 MPa, 0.5, respectively and E_1 = 13027.5 MPa by Eq. (27) of rule of mixtures and E_r = 9146.305 MPa, G_r = 3332.835 MPa by Eqs. 26 and 28 and μ_{random} equals 0.37 by Eq. (30).

For plantain empty fruit bunch fiber reinforced composites, where E_f, V_{fr}, E_{rm}, V_{rm} = 27344 MPa, 0.5, 2500 MPa, 0.5, respectively and by Eq. (28) of rule of mixtures and E_r = 9990.10 MPa, G_r = 3622.99 MPa by Eqs. 27 and 29 and v_{random} equals 0.38 by Eq. (30).

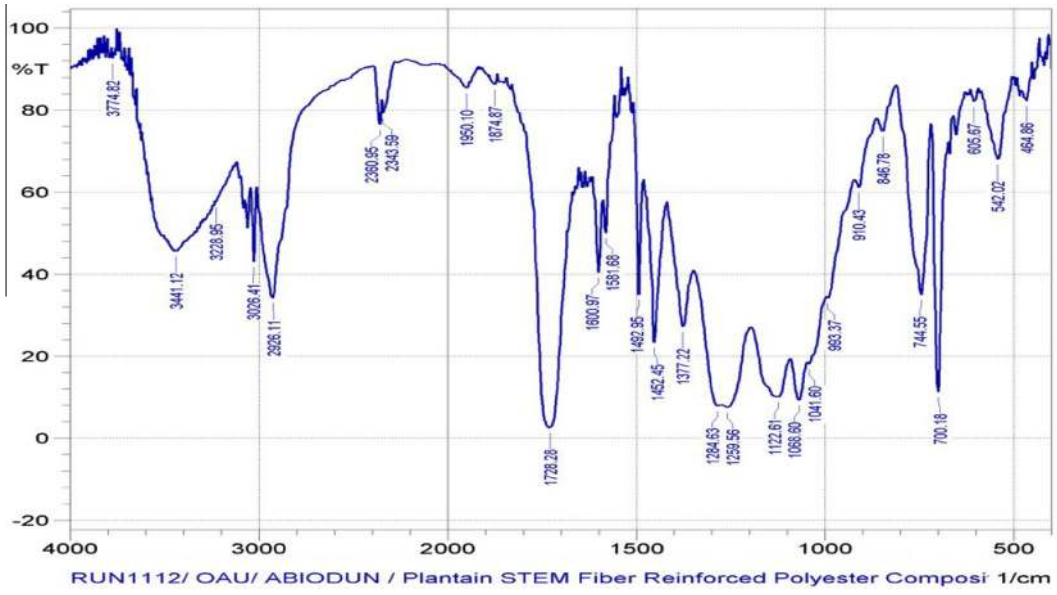

Figure 13 FTIR spectra of plantain stem fiber reinforced composites.

3.5. Computation of Poisson's ratio for the fibers

It has been reported that the lateral strain is 3–4 times less than axial strain, i.e.

$$\varepsilon_1 + 4\varepsilon_1 = \varepsilon \tag{31}$$

where ε is the axial or longitudinal strain and ε_1 is the lateral or transverse strain. The coefficient of lateral deformation, Poisson's ratio is expressed in Belyaev (1979) as

$$v = \frac{\text{lateral strain}}{\text{axial strain}} \tag{32}$$

Poisson's ratio is therefore the slope obtained by plotting lateral strain against axial strain. The slope of experimental or axial strain/5 plotted on the vertical axis and experimental strain on the horizontal axis gives Poisson's ratio of fibers as 0.20 for PEFBFRP and the PPSFRP, respectively. These are used with the rule of mixture equation to compute the respective composite Poisson's ratio in the fiber direction (Crawford, 1998). This equation can be expressed as

$$v_c = v_f V_{fr} + v_m V_{rm} \tag{33}$$

Poisson's ratios of the composites in fiber direction are therefore evaluated as 0.29 for both PEFBFRP and PPSFRP, respectively.

4. Computation of orthogonal material response with ANSYS

4.1. ANSYS finite element orthogonal deformation results for PEFBFRP at 50, 90, 10 sample settings

4.1.1. ANSYS finite element orthogonal deformation results for PPSFRP at 50, 90, 10 sample settings

4.1.1.1. Failure predictions with stress theories and specification of safety. Computation of principal stresses is based on Eq. (21) and that of orthogonal stress results of the ANSYS results, so that by putting the orthogonal stress results of nodes 30 and 100 of Tables 9 and 10 in Eq. (21) the following cubic equations for principal stresses for PEFBFRP and PPSFRP are obtained

$$\sigma^3 - 51.4274\sigma^2 + 503.3276\sigma - 445.3387 = 0 \tag{34}$$

$$\sigma^3 - 45.5183\sigma^2 + 386.0238\sigma - 890.3067 = 0 \tag{35}$$

The solution of Eqs. 34, 35 resulted to the principal stresses of the composite as presented in Tables 11 and 12

The failure yield stress S_y is evaluated with Eqs. (23)–(25) and presented in Table 11.

4.2. Estimation of transverse and longitudinal stresses of composite at failure

By using the values of the orthogonal stresses of Tables 9 and 10 at nodes 30 and 100 the orthogonal stresses are transformed to composite axis and the longitudinal and transverse stresses of the composites are evaluated and presented in Table 13.

It must be noted that composite failure stress determined during tensile test is the ultimate strength of composite in the transverse direction while the ultimate strength of composite in the longitudinal or in the direction of alignment of fibers is usually determined through the rule of mixtures. These stresses aid the determination of occurrence of yielding.

Halpin–Hill Criterion is an empirical criterion that defines failure as occurring if

$$\left(\frac{\sigma_{1\theta}}{S_{1u}}\right)^2 + \left(\frac{\sigma_{2\theta}}{S_{2u}}\right)^2 + \left(\frac{\tau_{12\theta}}{\tau_{12u}}\right)^2 \geq 1 \tag{36}$$

By employing the values of Tables 12 and 13 in Eq. (36) where $\tau_{12u} = \tau_{max} = \tau_{1/3}$, Eq. (36) is evaluated for PEFBFRP and PPSFRP, respectively as

$$\left(\frac{1.0944}{410.15}\right)^2 + \left(\frac{38.772}{37.3397}\right)^2 + \left(\frac{1.9777}{19.3100}\right)^2 = 1.10 \tag{37}$$

$$\left(\frac{6.0978}{288.10}\right)^2 + \left(\frac{35.283}{33.1330}\right)^2 + \left(\frac{0.000}{15.5700}\right)^2 = 1.13 \tag{38}$$

Since the values from computations of Eq. (36) gave 1.10 and 1.13 for composites of PEFBFRP and PPSFRP respectively and are more than unity (1), then failure is likely to occur and yield stresses need to be specified for the two materials.

Table 1 American society of testing and materials specifications.

Test	Standard	Specification for sample (mm)
Flexural	ASTM D790-10	$300 \times 19.05 \times 3.175$ mm
Tensile	ASTM D638-10	$150 \times 19.05 \times 3.2$ mm
Hardness	ASTM E10-12	$25 \times 25 \times 10$ mm
Charpy impact	ASTM A370	$55 \times 10 \times 10$ mm

Sources: ASTM A370 standard test methods and definitions for mechanical testing of steel products, ASTM E10-12 standard test method for brinell hardness of metallic materials, ASTM D638-10 standard test method for tensile properties of plastics, ASTM D790-10 standard test methods for flexural properties of unreinforced and reinforced plastics and electrical insulating materials.

Table 2 Theoretical volume of mold and volume of composite for sample replication.

Test	Standard	Specification for sample (mm × mm × mm)	Volume of mold (mm^3)	Volume of composite V_c (mm^3)
Tensile	ASTM D638-10	$150 \times 19.05 \times 3.2$ mm	$300 \times 300 \times 12 = 1080000$	$300 \times 300 \times 3.2 = 288000$

Source: ASTM D638-10 (ASTM, 0000).

4.3. Material characterization with FTIR spectroscopy

The FTIR spectroscopy measures the intensity of light absorbed or emitted by a material at a particular wave length which is related to some functional groups in the material. Nondestructive tests of Fourier transform infrared spectroscopy (FTIR) were carried out on plantain fibers and composites of plantain to establish fiber modification with treatments that improved the strengths of fibers and composites. It must be recalled that low strength properties and water absorption which are addressed by fiber modification limit the application of natural fibers.

As seen in Fig. 10, the strong peak 3406.40 cm^{-1} is characteristic of hydrogen-bonded –OH stretching vibration; the peak observed at 3406.40 cm^{-1} in untreated plantain empty fruit bunch fibers indicates the presence of intermolecular hydrogen bonding and tends to shift to higher absorbency values in treated fibers as shown in Fig. 11, similar observations have been reported in earlier works by Clemsons et al. (1992), Clemsons et al. (1992) and Rowell (1991). The peak at 2920.32 cm^{-1} is due to CH stretching vibrations (Mittal, 2000) and the peak at 1043.52 cm^{-1} is a characteristic of C–O– symmetric stretching vibration in cellulose, hemicellulose and minor lignin contribution (Lu and Drazel, 2010).

As can be seen in Fig. 11, the intensity of the peak around 3416.05 cm^{-1} which is evidence of OH band is increased after treatment of plantain fibers, this increment according to Liu et al. (2012) may be due to part of hydrogen bond and lignin that was broken during treatment, thus leading to an increase in the amorphous part in cellulose and release of more hydroxyl groups. The intensity of the band around 1759.14 cm^{-1} also increased due to the formation of ester band from the reaction between OH group and benzoylchloride (Agrawal et al., 2000). A strong peak at 1759.14 cm^{-1} in the FTIR spectrum indicates the presence of the acetyl group in the fiber. The intensity peak at 1058.96 cm^{-1} is increased after fiber treatment, which is an overlap of Si–O–Si band and C–O stretching of plantain fiber (Lu and Drazel, 2010; Agrawal et al., 2000).

From Fig. 12, the peak at 2926.11 cm^{-1} is due to C–H symmetric stretching. In the double bond region, a shoulder peak range at 1950.10 cm^{-1} in the spectrums is assigned to the C═O stretching of the acetyl and uronic ester (Bledzki et al., 2010).

The peak at about 2926.11 cm^{-1} in Fig. 13 is due to the C–H asymmetric stretching from aliphatic saturated compounds. This stretching peak is corresponding to the aliphatic moieties in cellulose and hemicelluloses (Liu et al., 2012). An aromatic functional group (C–C stretch in ring) was observed from the absorption band 1600.97 and 1492 cm^{-1}. A hydroxyl group was observed for both peaks from the absorption band 3774.82–3441.12 cm^{-1}. The carbonyl region (1874.87–1728.28 cm^{-1}) reveals probably the presence of the carbonyl group.

Table 3 Design variables for plantain empty fruit bunch fiber composite tensile tests.

V_{fr}	V_f (mm^3)	M_f (g)	V_R (mm^3)	M_R (g)	V_c (mm^3)
0.1	28800	10.200	259200	311.04	288000
0.2	57600	20.400	230400	276.48	288000
0.3	86400	30.599	201600	241.92	288000
0.4	115200	40.798	172800	207.36	288000
0.5	144000	50.998	144000	172.8	288000
0.6	172800	61.197	115200	138.24	288000
0.7	201600	71.397	86400	103.68	288000
0.8	230400	81.597	57600	69.12	288000

Table 4 Design variables for plantain pseudo stem fiber composite tensile tests.

V_{fr}	V_f (mm^3)	M_f (g)	V_R (mm^3)	M_R (g)	V_c (mm^3)
0.1	28800	11.008	259200	311.04	288000
0.2	57600	22.016	230400	276.48	288000
0.3	86400	33.024	201600	241.92	288000
0.4	115200	44.032	172800	207.36	288000
0.5	144000	55.039	144000	172.8	288000
0.6	172800	66.047	115200	138.24	288000
0.7	201600	77.055	86400	103.68	288000
0.8	230400	88.063	57600	69.12	288000

Table 5 Mechanical properties of plantain fiber.

Plantain part	Young modulus (MPa)	UTS (MPa)	Strain (%)	Density (kg/m^3)
Pseudostem	23555	536.2	2.37	381.966
Empty Fruit Bunch	27344	780.3	2.68	354.151

Source: Okafor, E.C., (Okafor et al., 2013) Ph.D thesis experimental data report.

Table 6 Mechanical properties of polyester resin.

Property	Polyester resin
Density (g/cm^3)	1.2–1.5
Young modulus (MPa)	2000–4500
Tensile strength (MPa)	40–90
Compressive strength (MPa)	90–250
Tensile elongation at break (%)	2
Water absorption 24 h at 20 °C	0.1–0.3
Flexural modulus (GPa)	11.0
Poisson's ratio	0.37–0.38

5. Discussion of results

Table 5 shows that the tensile properties of PEFBFRP such as modulus of composite and tensile strength of composite are higher than that of PPSFRP in the fiber direction when the rule of mixture equation is applied with the basic properties of reinforcing fibers and matrix. Figs. 2 and 3 express the variation of transverse moduli of composites with volume fraction of fibers while giving the average values of transverse mooduli at 50% volume fraction estimated with rule of mixtures, Brintrup and Halpin–Tai equations as 6818 and 7031 MPa, respectively for PPSFRP and PEFBFRP.

Fig. 4 and Table 9 show the orthogonal stresses with the maximum value at node 30 for PEFBFRP. Figs. 5 and 6 exhibit the maximum displacement and strain for PEFBFRP as 0.26 mm and 0.004 while Fig. 7 is a vector plot depiction of maximum degree of freedom as 0.27 for PEFBFRP. Fig. 8 and Table 10 show the maximum orthogonal stress for PPSFRP as 35.283 MPa while Fig. 9 is a vector depiction of maximum degree of freedom for PPSFRP as 0.25 mm. Table 11 expresses the principal stresses for both PEFBFRP and PPSFRP and gives the yield stresses for PFRP as 33.69 and 29.24 MPa for PEFBFRP and PPSFRP, respectively. Table 12 summarizes the basic physical and mechanical properties of PFRP evaluated in this study while Table 13 exhibits the composite direction stresses. Comparatively, the mechanical properties of natural fiber reinforced composites tested for engineering applications by Samuel et al. (2012) showed that glass laminate has the maximum tensile strength of 63 MPa while the ukam plant fiber laminate has the maximum tensile strength of 16.25 MPa; according to Satynarayana et al. (1987) the observed properties can be related to the internal structure and chemical composition of the fibers.

It was established that while the PEFBFRP carries 38.772 MPa, PPSFRP carries 35.283 MPa stresses equivalent to the ultimate tensile strength of the composites with respect

Table 9 ANSYS finite elements results for PEFBFRP-50% 90° (10) sample settings.

NODE	SX	SY	SZ	SXY	SYZ	SXZ
1	37.340	0.32030E-06	10.829	−0.43229E-06	0.0000	0.0000
2	37.340	0.13285E-06	10.829	0.16822E-06	0.0000	0.0000
4	37.340	−0.12616E-08	10.829	0.48565E-06	0.0000	0.0000
26	36.328	−0.47302E-01	10.522	0.14818	0.0000	0.0000
28	35.575	−0.38033E-01	10.306	0.19353E-01	0.0000	0.0000
30	38.772	1.0944	11.561	−1.9777	0.0000	0.0000
32	38.772	1.0944	11.561	1.9777	0.0000	0.0000
564	37.340	−0.35800E-06	10.829	0.65936E-06		
565	37.340	−0.97078E-06	10.829	−0.20651E-05		

Table 10 ANSYS finite elements results for PPSFRP-50% 90° (10) sample settings.

NODE	SX	SY	SZ	SXY	SYZ	SXZ
1	33.133	0.54789E-07	3.3133	−0.71909E-07	0.0000	0.0000
2	33.133	0.54265E-07	3.3133	0.71931E-07	0.0000	0.0000
60	33.133	−0.21030E-08	3.3133	−0.56613E-07	0.0000	0.0000
98	32.444	−0.66660	3.1778	0.50614	0.0000	0.0000
100	35.283	6.0978	4.1381	0.31273E-07	0.0000	0.0000
102	32.444	−0.66660	3.1778	−0.50614	0.0000	0.0000
564	33.133	−0.15509E-06	3.3133	0.32077E-06	0.0000	0.0000
565	33.133	−0.15613E-06	3.3133	−0.32084E-06	0.0000	0.0000

Table 11 Computed limit stresses for composites of PFRP.

Composites	Principal normal stress (MPa)			Maximum principal shear stress (MPa)	Yield stress		
					DET	MSST	MNST
	σ_1 (MPa)	σ_2 (MPa)	σ_3 (MPa)	$\tau_{1/3}$	S_y (MPa)	S_y (MP)	S_y (MPa)
PEFBFRP	37.80	14.44	−0.82	19.31	33.69	38.62	37.80
PPSFRP	35.30	6.06	4.16	15.57	29.24	31.13	35.30

Please cite this article in press as: Ihueze, C.C. et al., Natural fiber composite design and characterization for limit stress prediction in multiaxial stress state. Journal of King Saud University – Engineering Sciences (2013), http://dx.doi.org/10.1016/j.jksues.2013.08.002

Table 12 Evaluated mechanical properties of plantain fibers and plantain fiber reinforced polyester composites.

Composites/fibers	Properties								
	S_{u1} (MPa)	S_{u2} (MPa)	S_y (MPa)	E_1 (MPa)	E_2 (MPa)	E (MPa)	v	τ_{max} (MPa)	G (MPa)
PEFBF	780.30	–	–	27,344	–	–	0.2	1812.575	11393.33
PEFBFRP	410.15	37.3397	33.69	14,922	7030.962	9990.10	0.38	19.3100	3622.99
PPSF	536.20	–	–	23,555	–	–	0.20	1561.4100	9814.58
PPSFRP	288.10	33.1330	29.24	13027.5	6817.175	9146.305	0.37	15.5700	3332.835

S_{u1}, S_{u2} are tensile strengths in the longitudinal and transverse directions, respectively.

Table 13 Stress transformation for composite orientation stresses.

Composites	Orthogonal stresses						Composite orientation stresses		
	SX	SY	SZ	SXY	SYZ	SXZ	$\sigma_{1\theta}$	$\sigma_{2\theta}$	$\tau_{12\theta}$
PEFBFRP	38.772	1.0944	11.561	−1.9777	0.000	0.0000	1.0944	38.772	1.9777
PPSFRP	35.283	6.0978	4.1381	0.0000	0.0000	0.0000	6.0978	35.283	0.000

to their transverse directions. Table 12 equally reports the tensile strength of PEFBFRP in the fiber direction as 410.15 MPa and for PPSFRP as 288.10 MPa while Chimekwene et al. (2012) studied on the mechanical properties of a new series of bio-composite involving plantain empty fruit bunch as reinforcing material in an epoxy based polymer matrix and found an optimal tensile strength of 243 N/mm^2 from the woven roving treated fiber orientation at a fiber volume fraction of 40%. Bisanda and Ansell, 1991 studied the mechanical properties of sisal fiber/polyester composites and found the tensile strength at 50% volume fraction to be 47.1 MPa; investigation on banana fiber reinforced polyester composites by Laly et al. (2003) gave the optimum content of fiber at 40%. The result of the current study however, is slightly higher than the results obtained by Myrtha et al. (2008) and Laly et al. (2003).

The FTIR spectra of fibers and composites are depicted in Figs. 10–13. There are irregular patterns of light intensity spectrum of PFRP as depicted in Figs. 12 and 13 and related to fiber spectra of Figs. 10 and 12. Figs. 10 and 11 show the absorbance peaks in the regions of 472.58 and 3406.4 cm^{-1} for untreated PEFPF and 418.57 and 3774.82 cm^{-1} for treated PEFBF showing that the fibers are modified while Figs. 12 and 13 show the absorbance peaks in the regions of 468.72 and 3435.34 cm^{-1} for PEFBFRP and 464.86 and 3774.82 cm^{-1} for PPSFRP. These correspond to ranges of 2966.62 and 3309.96 cm^{-1} for PEFBFRP and PPSFRP, respectively. These correspond to absorbed intensity ranges of 85.98–48.12 = 37.86 and 92.687–82.311 = 10.376 for PEFBFRP and PPSFRP, respectively. The average intensities of the untreated and treated fibers are estimated for plantain empty fruit bunch fibers as 55.35 and 65.015 showing the influence of fiber modification on light absorption. The average light intensities for PEFBFRP and PPSFRP are 45.47304 and 45.77, respectively. This signifies that the composites may have similar properties but PPSFRP may be more porous than PEFBFRP. In general, the FTIR study provides chemical characteristics of the new material as illustrated in Figs. 10–13. It has proved to be useful in analyzing chemical and structural changes that occur in plantain fiber components due to different treatments, this is evident as the intensity of the peak around 3416.05 cm^{-1} in Fig. 11 which is a characteristic of OH band is increased after treatment, this increment according to Liu et al. (2012) may be due to part of hydrogen bond and lignin that was broken during treatment. Similar observations have been reported in earlier works by Clemsons et al. (1992), Mallari et al. (1990) and Rowell (1991). The design of a unidirectional fiber composite will be based on the properties of composites as related to the transverse direction.

6. Conclusion

This study concludes that PFRP composite physical and mechanical properties relevant in the design of components of structures are comparable to the conventional glass fiber reinforced plastics like E glass/epoxy (GFRP), E glass polyester (GFRP), Kevlar 49/epoxy (KFRP) and carbon/epoxy (CFRP) with PEFBFRP having higher mechanical qualities than PPSFRP. Above all,

1. The application of PFRP is limited by transverse properties of plantain fibers and the matrix properties since the rule of mixtures relied on the volume fraction of fibers and matrix to estimate composite properties in the fiber direction.
2. The tensile strength of PEFBFRP in the transverse and longitudinal(fibers) directions is 37.3397 and 410.15 MPa, respectively while that of PPSFRP is 33.133 and 288.10 MPa, respectively
3. The yield strength of PEFBFRP is 33.69 MPa while that of PPSFRP is 29.24 MPa.
4. Above all the PEFBFRP with average light absorbance peak of 45.47 was found to have better mechanical properties than the PPSFRP with average light absorbance peak of 45.77.
5. It is recommended that reinforcement combinations that improve the directional response of PFRP such as plain weave fiber arrangement (fabric, cloth or mat) in which the strength is uniform in both directions should be encouraged.

Please cite this article in press as: Ihueze, C.C. et al., Natural fiber composite design and characterization for limit stress prediction in multiaxial stress state. Journal of King Saud University – Engineering Sciences (2013), http://dx.doi.org/10.1016/j.jksues.2013.08.002

Appendix A.

Tables 1–6, Tables 9–13

References

Agbo, S., 2009, Modelling of Mechanical Properties of a Natural and Synthetic Fiber-Reinforced Cashew nut Shell Resin Composites, M.Sc. Thesis, Department of Mechanical Engineering, University of Nigeria.

Agrawal, R., Saxena, N.S., Sharma, K.B., Thomas, S., Sreekala, M.S., 2000. Activation energy and crystallization kinetics of untreated and treated oil palm fiber reinforced phenol formaldehyde composites. Mater. Sci. Eng., A 277 (1–2), 77–82.

Ahmed, S., 2004. The Survey of Nigeria Agriculture by Raw Materials Research and Development Council (RMRDC), 123.

ASTM D638-10 Standard Test Method for Tensile Properties of Plastics.

Belyaev, N.M., 1979. Strength of Materials. MIR publishers, MOSCO.

Bisanda, E.T.N., Ansell, M.P., 1991. The effect of silane treatment on the mechanical and physical properties of sisal–epoxy composites. Compos. Sci. Technol. 41, 165–178.

Bledzki, A.K., Mamuna, A.A., Volk, J., 2010. Physical chemical and surface properties of wheat husk, rye husk and soft wood and their polypropylene composites. Compos. Part A 41, 480–488.

Brahmakumar, M., Pavithran, C., Pillai, R.M., 2005. Coconut fibre reinforced polyethylene composites: effect of natural waxy surface layer of the fibre on fibre/matrix interfacial bonding and strength of composites. Mater. Processing Technol. 3–4 (65), 563–569.

Calado, V., Barreto, D.W., Dalmeida, J.R.M., 2000. The effect of a chemical treatment on the structure and morphology of coir fiber. J. Mater. Sci. Lett. 19, 2151–2153.

Chen, A.S., Matthews, F.L., 1993. A review of multiaxial/biaxial loading tests for composite materials. Composites 24 (5), 395–406.

Chimekwene, C.P., Fagbemi, E.A., Ayeke, P.O., 2012. Mechanical properties of plantain empty fruit bunch fiber reinforced epoxy composite. Int. J. Res. Eng., IT Social Sci. 2 (6), 86–94.

Clemsons, C., Young, R.A., Rowell, R.M., 1992. Moisture sorption properties of composite boards from esterified aspen fiber. Wood Fiber Sci. 24 (3), 353–363.

Crawford, R.J., 1998. Plastics Engineering, third ed. Butterwoth-Heinemann, Great Britain.

El-Hajjar, R., Haj-Ali, R., 2004. In-plane shear testing of thick-section pultruded FRP composites using a modified Arcan fixture. Compos. Part B: Eng. 35B (5), 421–428.

Food Agriculture Organization, 1990. Production Yearbook 1990. FAO, Rome.

Food and Organization, 2006. Production Yearbook 2006. FAO, Rome.

Ghali, L., Msahli, S., Zidi, M., Sakli, F., 2011. Effects of fiber weight ratio, structure and fiber modification onto flexural properties of luffa-polyester composites. Adv. Mater. Phys. Chem. 2011 (1), 78–85.

Haj-Ali, R., Kilic, H., 2002. Nonlinear behavior of pultruded FRP composites. Compos. Part B: Eng. 33 (3), 173–191.

Haj-Ali, R.M., Muliana, A.H., 2003. A micromechanical constitutive framework for the nonlinear viscoelastic behavior of pultruded composite materials. Int. J. Solids Struct. 40 (5), 1037–1057.

Haj-Ali, R.M., Muliana, A.H., 2004. Numerical finite element formulation of the Schapery non-linear viscoelastic material model. Int. J. Num. Meth. Eng. 59 (1), 25–45.

Hall, Derek, 1981. An Introduction to Composite Material. Cambridge University press, Australia.

Hamrock, B.J., Jacobson, B.O., Schmid, S.R., 1999. Fundamentals of Machine Elements. WCB/McGraw-Hill, pp. 290–292.

Hinton, M.J., Soden, P.G., 2002. A comparison of the predictive capabilities of current failure theories for composite laminates, judged against experimental evidence. Compos. Sci. Technol. 62, 1725–1797.

Hinton, M.J., Kaddour, A.S., Soden, P.D., 2004. Failure Criteria in Fibre Reinforced Polymer Composites: The World-Wide Failure Exercise. A Composite Science and Technology Compendium. Elsevier.

Kilic, H., Haj-Ali, R., 2003. Progressive damage and nonlinear analysis of pultruded composite structures. Compos. Part B: Eng. 34 (3), 235–250.

Laly, A. Pothana, Oommenb, Zachariah, Thomas, Sabu, 2003. Dynamic mechanical analysis of banana fiber reinforced polyester composites. Compos. Sci. Technol. 63 (2), 283–293.

Liu, Y., Jang, J., Zheng, Y., Wang, A., 2012. Adsorption of methylene blue by kapok fiber treated by sodium chlorite optimized with response surface methodology. Chem. Eng. J. 184, 248–255.

Lu, J., Drazel, L.T., 2010. Microfibrillated cellulose/cellulose acetate composites: effect of surface treatment. J. Polym. Sci., Part B: Polym. Phys. 48 (2), 153–161.

Mallari, V.C., Fukuda, K., Morohoshi, N., Haraguchi, T., 1990. Biodegradation of particleboard II. Decay resistance of chemically modified particleboard. Mokuzai Gakkaishi 32 (2), 139–146.

Mittal, K.L., 2000. In: Silanes and Other Coupling Agents, vol. 2. VSP, Utrecht, The Netherlands.

Myrtha, K., Holia, O., Dawam, A.A.H., Anung, S., 2008. Effect of oil palm empty fruit bunch fiber on the physical and mechanical properties of fiber glass reinforced polyester resin. J. Biol. Sci. 8 (1), 101–106.

Okafor, E.C., 2013. Unpublished Ph.D thesis, Department of Industrial and Production Engineering, Nnamdi Azikiwe University, Awka, Nigeria.

Oladele, I.O., Omotoyinbo, J.A., Adewara, J.O.T., 2010. Investigating the effect of chemical treatment on the constituents and tensile properties of sisal fibre. J. Miner. Mater. Charact. Eng. 9 (6), 569–582.

Olsson, R., 2011. A survey of test methods for multiaxial and out-of-plane strength of composite laminates. Compos. Sci. Technol.. http://dx.doi.org/10.1016/j.compscitech.2011.01.022.

Rowell, R.M., 1991. Natural Composites, Fiber Modification. In: Lee, S.M. (Ed.), International Encyclopedia of Composites. VHC, New York.

Rowell, R.M., 1998. Property enhanced natural fiber composite materials based on chemical modification. In: Prasad, P.N. et al. (Eds.), Science and Technology of Polymers and Advanced Materials. Plenum Press, New York.

Samuel, O.D., Agbo, S., Adekanye, T.A., 2012. Assessing mechanical properties of natural fibre reinforced composites for engineering applications. J. Miner. Mater. Charact. Eng. 11 (1), 1–5.

Satynarayana, K., Pillai, C.K.S., Sukumaran, K., Rohatgi, P.K., Vijayan, K., 1987. Structure property studies of fiber from various parts of the coconut tree. J. Mater. Sci. 22, 3167–3172.

Shigley, J.E., Mischke, C.R., 1989. Mechanical Engineering Design, fifth ed. McGraw-Hill.

Soden, P.D., Hinton, M.J., Kaddour, A.S., 2002. Biaxial test results for strength and deformation of a range of e-glass and carbon fibre reinforced composite laminates: failure exercise benchmark data. Compos. Sci. Technol. 62, 1489–1514.

Stamboulis, A., Baley, C., 2001. Composites Part A: Applied Science and Manufacturing. Effects of Environ-mental Conditions on Mechanical and Physical Properties of Flax Fibres 32, 1105–1115.

Venkataswamy, K.G., Pillai, C.K.S., Prasad, V.S., et al, 1987. Effect of weathering on mechanical properties of midribs coconut leaves. J. Mater. Sci. 22, 3167–3317.

Westman, M.P., Fifield, L.S., Simmons, K.L., Laddha, S.G., Kafentzis, T.A., 2010. Natural Fiber Composites: A Review. Pacific Northwest National Laboratory.

Xiaoya, C., Qipeng, G., Yongli, M., 1998. J. Appl. Polym. Sci. 69, 1891–1899.

Please cite this article in press as: Ihueze, C.C. et al., Natural fiber composite design and characterization for limit stress prediction in multiaxial stress state. Journal of King Saud University – Engineering Sciences (2013), http://dx.doi.org/10.1016/j.jksues.2013.08.002